ICASSP 2023 - 2023 IEEE International Conference on Acoustics, Speech and Signal Processing (ICASSP) | 978-1-7281-6327-7/23/$31.00 ©2023 IEEE | DOI: 10.1109/ICASSP49357.2023.10096906

UNLIMITED SAMPLING OF FRI SIGNALS INDEPENDENT OF SAMPLING RATE

Ruiming Guo and Ayush Bhandari

Dept. of Electrical and Electronic Engg., Imperial College London, SW7 2AZ, UK.
Email: {ruiming.guo,a.bhandari}@imperial.ac.uk or ayush@alum.mit.edu

ABSTRACT

To achieve High Dynamic Range (HDR) sensing, the Unlimited Sampling Framework (USF) was recently proposed. In the USF, modulo encoding of the continuous-time input signal prevents the analog-to-digital converter (ADC) from saturation. For recovering the HDR signal from folded samples, reconstruction algorithms are utilized. Current USF pipeline is highly focused on bandlimited signal classes and requires considerable oversampling. In contrast, in this paper, we consider non-bandlimited signals, in particular, sparse inputs with finite-rate-of-innovation (FRI). By devising a novel, dual-channel modulo sampling architecture we show that, surprisingly, sparse signal recovery from modulo samples can be performed independent of the sampling rate. We validate the effectivity of our sampling scheme and show that perfect signal reconstruction is achieved up to machine precision.

Index Terms— ADC, modulo, non-linear reconstruction, sampling, sparse recovery, super-resolution.

1. INTRODUCTION

Digital acquisition of signals is the stepping stone for a wide variety of modern world applications. Guided by Shannon-Nyquist sampling framework, a point-wise signal acquisition scheme is implemented using the so-called analog-to-digital convertor (ADC). Shannon sampling theory is mature technology and has been thoroughly studied for decades [1], covering both the theoretical underpinnings of sampling framework as well as the algorithmic strategies to overcome distortions arising in practice, *e.g.* system noise and quantization. Beyond these distortions, a fundamental bottleneck that inevitably arises in practice is the dynamic range (DR) of the ADC—samples suffer from signal clipping or saturation when the DR of the ADC and signal of interest are not matched. To overcome this fundamental barrier, recently, the Unlimited Sampling Framework (USF) [2–7] was introduced as an alternative solution to Shannon-Nyquist sampling framework. The USF allows for a High Dynamic Range (HDR) capture, *e.g.* as shown in [5], signals as large as $25\times$ the ADC threshold can be recovered in practice. Furthermore, for a given bit-budget, since the range of modulo operator is much lower than the ambient, HDR signal, modulo ADCs produce samples with higher quantization resolution [3]. The implication being, in applications such as Radars [8], one can achieve higher signal sensitivity due to lower quantization noise in modulo ADCs.

In contrast to the conventional paradigm—*capture first, process later*—the USF utilizes a joint design of hardware and algorithms to bridge the gap between the theory and practical implementation of traditional sampling framework. Traditionally, the hardware and reconstruction algorithms are disentangled from each other. While in the USF, a modulo non-linearity defined by

$$\mathscr{M}_\lambda : g \mapsto 2\lambda \left(\left[\!\left[\frac{g}{2\lambda} + \frac{1}{2} \right]\!\right] - \frac{1}{2} \right), \quad [\![g]\!] \stackrel{\mathrm{def}}{=} g - \lfloor g \rfloor, \quad \lambda \in \mathbb{R}^+ \tag{1}$$

where $\lfloor g \rfloor = \sup \{ k \in \mathbb{Z} | \, k \leqslant g \}$ (floor function), is embedded in the sampling pipeline before capturing point-wise samples. In doing so, an arbitrary HDR continuous-time signal is folded back into the ADC's dynamic range $[-\lambda, \lambda]$, thus the clipping problem can be eliminated. Together with a point-wise sampling, this constructs the modulo ADC architecture, as shown in Fig. 1. By using novel recovery algorithms, the samples arising from $\mathscr{M}_\lambda(\cdot)$ operator can be unfolded; this enables recovery of HDR signal from its low dynamic range samples. The effectiveness of USF on hardware experiments has been demonstrated via modulo ADCs in [5]. Applications of the USF include, sensor array processing [9]; sparse signal reconstruction [6, 10]; HDR imaging [11]; tomography [12], massive MIMO [13], etc.

Motivation. Current works on the USF are predominantly focused on bandlimited/smooth signal classes. Apart from the above-mentioned papers, we refer to the following works [7, 14–18] that develop recovery algorithms for bandlimited functions. Alternatively, an interesting class of signals is that of *finite-rate-of-innovation* or FRI signals [19–21]. Due to the widespread applications of sparse and FRI signals, modulo sampling of such signal classes has been discussed in [10]. Recently, a robust algorithm with its hardware validation in the context of time-of-flight imaging was presented in [6]. These initial works convey the promise of sparse super-resolution problem but are currently limited by,

1) **Bandlimited Sampling Kernels.** In practice, kernels may be time-localized [20] and such functions are optimally modeled by time-limited pulses.
2) **Sampling-Rate.** Modulo folding of signals typically requires a sampling rate that is higher than the rate-of-innovation. While this is expected because it is natural to trade-off dynamic range with oversampling, in some cases *e.g.* [10], the sampling rate is inversely proportional to the modulo threshold.

These two aspects motivate new USF architectures that can handle time-limited kernels and algorithms that can reconstruct signals acquired at their rate-of-innovation.

Contributions. The main contributions of our work are as follows.

1. We propose a novel acquisition pipeline which relies on a dual-channel sampling architecture. Surprisingly, this simple acquisition pipeline results in a sampling scheme which is free of any sampling rate requirement.

The work of the authors is supported by the UK Research and Innovation council's FLF Program "Sensing Beyond Barriers" (MRC Fellowship award no. MR/S034897/1). Further details on Unlimited Sensing and upcoming materials on *reproducible research* are available via https://bit.ly/USF-Link.

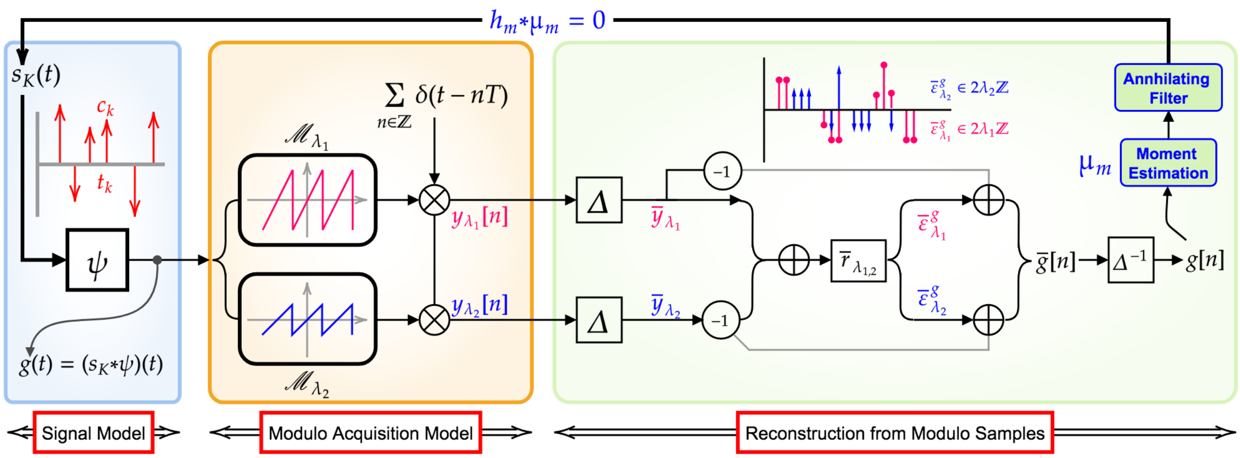

Fig. 1. Flowchart of the Unlimited Sampling scheme of FRI signals.

2. Our sampling scheme can handle time–limited or compactly supported kernels. This is very different from previous works which were based on bandlimited kernels [6, 10].
3. Our recovery method is theoretically guaranteed and leads to perfect signal reconstruction. This enables super-resolution of signal parameters from modulo samples (see Fig. 4).

Related Research Efforts and Context. Our previous papers [6, 10] formulated the sparse or FRI signal recovery problem from modulo samples but these works were restricted to bandlimited sampling kernels and the sampling rate was implicitly linked to the dynamic range of the signal (relative to the modulo ADC). Apart from these works, compressive sensing from modulo samples has been studied in [22–24] but these methods do not apply to our problem setup.

2. SAMPLING PIPELINE AND PROBLEM FORMULATION

In this paper, we focus on the modulo sampling strategy for non-bandlimited signal classes, in particular, FRI signals [19]. Our novel sampling pipeline allows for a tighter signal model and enables perfect recovery for non-bandlimited signals. Fig. 1 depicts the modulo sampling process of sparse signals: a stream of Diracs $s_K(t)$

$$s_K(t) = \sum\nolimits_{k=0}^{K-1} a_k \delta(t - t_k) \tag{2}$$

is filtered with a filter $\psi(t)$ of compact support ($\psi(t) = 0, \forall\ |t| \geqslant P$), which yields the output signal

$$g(t) = (s_K * \psi)(t) = \sum\nolimits_{k=0}^{K-1} a_k \psi(t - t_k). \tag{3}$$

Such signals are called signals with finite-rate-of-innovation since they are completely described by a finite number of free parameters per unit of time.

In the USF, modulo non-linearity is applied in the continuous domain; *i.e.* $g(t)$ is folded via the centered modulo operation in (1). This results in the folded signal $\mathscr{M}_\lambda(g(t))$ (see Fig. 1) which is then uniformly sampled, leading to a stream of modulo samples

$$y[n] = \mathscr{M}_\lambda(g(nT)) = \mathscr{M}_\lambda\Big(\sum\nolimits_{k=0}^{K-1} a_k \psi(nT - t_k)\Big) \tag{4}$$

where T is the sampling step and the filter $\psi(t)$ is of compact support P (*e.g.* splines).

3. UNLIMITED SAMPLING OF SPARSE SIGNALS

As the input signal $g(t)$ is clearly non-bandlimited, recovery approaches developed to modulo sampling, e.g. Fourier domain partitioning [6] and high-order finite difference [2, 3], cannot be applied in our context. This motivates the development of new methods.

Modular Decomposition Representation. Our starting point is the modular decomposition property [3] which allows us to write,

$$g = \mathscr{M}_\lambda(g) + \varepsilon^g, \quad \varepsilon^g(t) = \sum\nolimits_{l=0}^{L-1} c_l \mathbb{1}_{\mathcal{D}_l}(t) \tag{5}$$

where $c_l \in 2\lambda\mathbb{Z}$, $\varepsilon^g(t)$ is the residue function and $\mathbb{1}_{\mathcal{D}}$ is the indicator function on domain D with $\cup_l \mathcal{D}_l = \mathbb{R}$. Denoting by $\underline{y}$ the finite difference of y, we have

$$\underline{y}[n] = \underline{g}[n] - \sum\nolimits_{l=0}^{L-1} c_l \delta[n - n_l], \quad n = 0, \cdots, N-2$$

where $\{n_l\}_{l=0}^{L-1}$ are the unknown folding instants—the locations where the modulo non-linearity yields. The triggering rate of n_l depends on the $\mathscr{M}_\lambda$–ADC threshold λ. For a certain dynamic range, smaller the λ, higher is the folding rate and larger is the number of spikes in (3). Obviously, both $\underline{g}[n]$ and $\underline{\varepsilon}^g[n]$ are non-bandlimited, resulting in aliasing in the Fourier domain. In order to separate the residue $\underline{\varepsilon}^g[n]$ out of $\underline{y}[n]$, we propose a new recovery scheme.

Modulo Sparse Recovery Via Residue Separation. The key idea of recovering $g[n]$ from $\underline{y}[n]$ is that the amplitudes of spikes $\{c_l\}_{l=0}^{L-1}$ are multiple times of the $\mathscr{M}_\lambda$–ADC threshold, i.e. $c_l \in 2\lambda\mathbb{Z}, l = 0, 1, \cdots L-1$. Before presenting the sampling theorem, we first introduce the following lemma:

Lemma 1. *Assume a sparse signal $g(t)$ sampled by two modulo ADCs with different thresholds λ_1 and λ_2, which gives rise to modulo samples $y_{\lambda_1}[n], y_{\lambda_2}[n]$. Then, the sparse samples $g[n]$ can be exactly recovered if λ_1/λ_2 is irrational.*

Proof. From (3), we have that

$$\underline{y}_{\lambda_1}[n] = \underline{g}[n] - \underline{\varepsilon}^g_{\lambda_1}[n], \ \underline{y}_{\lambda_2}[n] = \underline{g}[n] - \underline{\varepsilon}^g_{\lambda_2}[n] \tag{6}$$

By computing the difference between $\underline{y}_{\lambda_1}[n]$ and $\underline{y}_{\lambda_2}[n]$, we obtain

$$\underline{r}_{\lambda_{1,2}} = \underline{\varepsilon}^g_{\lambda_2}[n] - \underline{\varepsilon}^g_{\lambda_1}[n] = \sum\nolimits_{l=0}^{L_1+L_2-1} c_l \delta[n - n_l] \tag{7}$$

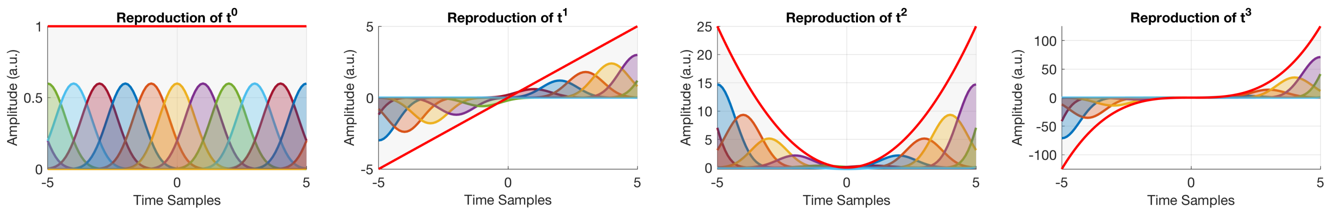

Fig. 2. Illustration of polynomial reproducing kernel. $\psi(t)$ is a cubic spline.

which is a sparse signal with weights $c_l = 2\lambda_2 p_l - 2\lambda_1 q_l, \{p_l, q_l\} \in \mathbb{Z}^2$. It suffices to show that, the mapping between c_l and $\{p_l, q_l\}$ is a injection, i.e.

$$2\lambda_2 p_l - 2\lambda_1 q_l = 2\lambda_2 p_{l'} - 2\lambda_1 q_{l'} \iff p_l = p_{l'}, q_l = q_{l'}$$

which follows from the fact that $\nexists \{p_l, q_l\} \in \mathbb{Z}^2$, s./t. $\lambda_1/\lambda_2 = p/q$.

Hence, $\{p_l, q_l\}$ can be uniquely recovered from c_l, which thereby leads to a perfect reconstruction of $\underline{\varepsilon}^g_{\lambda_1}[n]$ and $\underline{\varepsilon}^g_{\lambda_2}[n]$. By applying anti-difference operator Δ^{-1}, the sparse samples $g[n]$ can then be perfectly recovered. This completes the proof of Lemma. 1. ∎

We emphasize that the dual-channel modulo sampling in Lemma. 1 results in an exact recovery of $g[n]$, which can be expressed as a sum of shifted kernels ψ. Retrieving the parameters $\{a_k, t_k\}$ from $g[n]$ essentially boils down to the sparse recovery using reproduction of polynomials [20], which leads to the following sampling theorem:

Theorem 1. *Let $g(t) = (s_K * \psi)(t)$ as defined in (3) where $\psi(t)$ is a compactly supported polynomial reproducing kernel. Let $y_{\lambda_m}[n], m = 1, 2$ be the modulo samples of $g(t)$ with distinct folding thresholds, $\lambda_1 \neq \lambda_2$. Provided that λ_1/λ_2 is irrational, $N \geqslant P \geqslant 2K$ guarantees a perfect reconstruction of $g(t)$.*

Proof. We present the proof of this theorem by constructing the solution to the problem. Let $\underline{r}_{\lambda_{1,2}} = \underline{y}_{\lambda_1} - \underline{y}_{\lambda_2}$ denote the difference between $\underline{y}_{\lambda_1}$ and $\underline{y}_{\lambda_2}$, which is a sum of at most $L_1 + L_2$ spikes as in (7). Its amplitudes are given by $c_l = 2\lambda_2 p_l - 2\lambda_1 q_l$. Provided that $c_l \neq 0$, $\{p_l, q_l\}$ can be exactly retrieved whenever λ_1/λ_2 is irrational. Hence, $\underline{g}$ can be recovered by removing the reconstructed residue using p_l, q_l from the modulo samples $\underline{y}_{\lambda_1}, \underline{y}_{\lambda_2}$. Furthermore, by applying the anti-difference operator, g can be recovered. Next, note that the compactly-supported ψ satisfies,

$$\mathrm{C}^m_n \circledast_T \overline{\psi}(t) = t^m, \quad 0 \leqslant m \leqslant P-1 \tag{8}$$

where $a_n \circledast_T \psi(t) = \sum_{n=0}^{N-1} a_n \psi(t - nT)$ denotes semi-discrete convolution, $\overline{\psi}(t) = \psi(-t)$. The polynomial reproduction property is visually illustrated in Fig. 2. Linearly combining g with coefficients C^m_n in (8), we obtain the new moment sequence:

$$\mu_m = \sum_{n=0}^{N-1} \mathrm{C}^m_n g[n] = \sum_{k=0}^{K-1} a_k \left(\mathrm{C}^m_n \circledast_T \overline{\psi}\right)(t_k) \overset{(8)}{=} \sum_{k=0}^{K-1} a_k t_k^m. \tag{9}$$

Let h_m with $m = 0, 1, \cdots, K$ be the filter with z-transform $\widehat{h}(z) = \sum_{m=0}^{K} h_m z^{-m} = \Pi_{k=0}^{K-1}(1 - t_k z^{-1})$, that is, its roots correspond to the Dirac locations t_k to be found. Then, it follows that h_m annihilates the observed sequence μ_m:

$$h_m * \mu_m = \sum_{i=0}^{K} h_i \mu_{m-i} = \sum_{k=0}^{K-1} a_k t_k^m \sum_{i=0}^{K} h_i t_k^{-i}. \tag{10}$$

Let $\mathbf{T}(\mu_\mathbf{m})$ denote the Toeplitz matrix. According to (10), $\mathbf{h} \in \ker \mathbf{T}(\mu_\mathbf{m})$ or $\mathbf{T}(\mu_\mathbf{m})\mathbf{h} = \mathbf{0}$ whenever $\mathbf{T}(\mu_\mathbf{m})$ is a rank-deficient. By solving the above linear system of equations, we find the filter coefficients h_m and then retrieve t_k by computing the roots of polynomial $\widehat{h}(z)$. It remains to estimate the Dirac amplitudes a_k which can be determined via least-squares fitting (9). Notice that the problem can be solved when there are at least as many equations as unknowns, implying that $P \geq 2K$. This completes the proof. ∎

Theorem 1 shows that spike recovery is related to its rate-of-innovation and is independent of the sampling step T. This enables sampling and reconstruction of $s_K(t)$ with critical sampling rate—the rate-of-innovation as shown in Sec. 6. An efficient implementation of our recovery method is outlined in Sec. 5.

4. MODULO SAMPLING WITH PRACTICAL FILTER

In this section, we show that the dual-channel sampling scheme also applies to *arbitrary time-limited* filters, mimicking what happens in practice. To do so, we express an arbitrary kernel, say $\phi(t)$, as a linear combination of time-limited sampling filter,

$$\phi(t) = \sum_{i=0}^{Q-1} \alpha_i \psi(t - q_i) \tag{11}$$

with $\{q_i, \alpha_i\}_{i=0}^{Q-1}$ known. Then, we have the following corollary:

Corollary 1. *Let $g(t) = (s_K * \phi)(t) = \sum_{k=0}^{K-1} a_k \phi(t - t_k)$ where $\phi(t) = \sum_{i=0}^{Q-1} \alpha_i \psi(t - q_i)$ (as in (11)). Given $N \geqslant \operatorname{supp}(\phi) \geqslant 2KQ$, $s_K(t)$ can be recovered from its dual-channel modulo samples.*

Proof. In view of $\mathrm{C}^m_n \circledast_T \overline{\psi}(t) = t^m$ (8), the arbitrary kernel ϕ also reproduces polynomials,

$$\mathrm{C}^m_n \circledast_T \overline{\phi}(t) = \sum_{i=0}^{Q-1} \alpha_i (t + q_i)^m. \tag{12}$$

The implication being, computing moments with C^m_n, results in,

$$\mu^\phi_m = \sum_{n=0}^{N-1} \mathrm{C}^m_n g[n] = \sum_{k=0}^{K-1} a_k \sum_{i=0}^{Q-1} \alpha_i (t_k + q_i)^m \tag{13}$$

which can be annihilated using the annihilation filter method described in Theorem 1. This results in the recovery of $\{a_k \alpha_i, t_k + q_i\}$. Moreover, with $\{\alpha_i, q_i\}$ known, it suffices to show that

$$\sum_{k=0}^{K-1} a_k \sum_{i=0}^{Q-1} \alpha_i e^{\jmath \frac{2\pi m}{N}(t_k + q_i)} = \sum_{k=0}^{K-1} a_k e^{\frac{2\pi m t_k}{N}} \sum_{i=0}^{Q-1} \alpha_i e^{\frac{2\pi m q_i}{N}} \tag{14}$$

where $\{a_k, t_k\}_{k=0}^{K-1}$ are the unknown parameters. The problem eventually amounts to retrieving frequencies from a sum of sinusoids, which again can be solved using the annihilation filter method in (10). This results in a perfect reconstruction of $s_K(t)$ from the dual-channel modulo samples. ∎

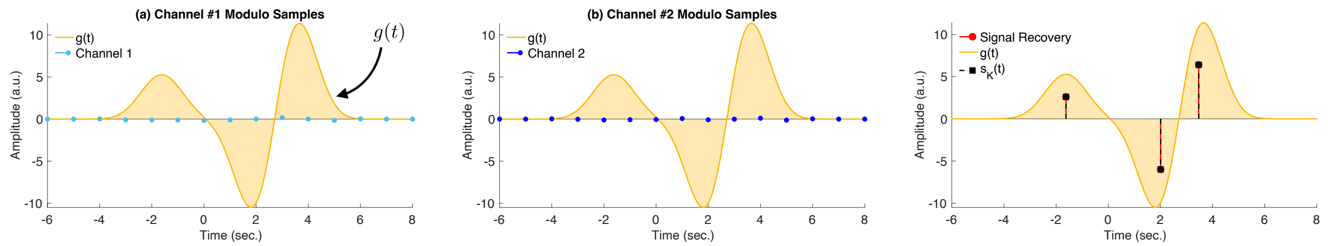

Fig. 3. Sparse Signal Recovery. Input $g(t)$ is composed of $K = 3$ spikes, $s_3(t)$, filtered with kernel $\psi(t)$ (B-spline with $P = 7$), leading to $\|g\|_\infty = 10$. The signal is acquired via our dual-channel modulo architecture with folding thresholds $\lambda_1 = 0.20$ and $\lambda_2 = 0.14$, respectively. The dynamic range of each channel is, $50.0\lambda_1, 70.7\lambda_2$ and hence the modulo samples seem to have negligible amplitudes. The modulo folding results in $L_1 = L_2 = 10$, per channel. Given ψ, with $N = 19$ samples, we reconstruct $s_3(t)$, with MSE $= 1.19 \times 10^{-16}$.

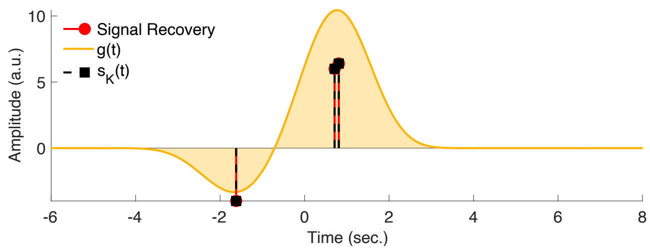

Fig. 4. Super-Resolution. We consider the case of closely separated spikes. With $N = 19$ samples, $L_1 = L_2 = 7$ folding instants we recover s_k with MSE $= 5.74 \times 10^{-15}$.

5. ALGORITHMIC SETTING

We develop the annihilation filter based procedure to reconstruct the sparse signal from dual-channel modulo samples. Below, we list the steps of our recovery method.

1. Given dual-channel modulo samples $y_{\lambda_1}[n], y_{\lambda_2}[n]$, we compute the difference $\underline{r}_{\lambda_{1,2}}$ in (7) using (6). As mentioned earlier, $\underline{r}_{\lambda_{1,2}}$ is a sum of spikes, for which its amplitudes map to a unique solution (p_l, q_l). This follows from the assumption that λ_1/λ_2 is irrational. Hence, $\underline{\varepsilon}^g_{\lambda_1}[n], \underline{\varepsilon}^g_{\lambda_2}[n]$ can be exactly recovered, and thereby $g[n]$ is reconstructed.
2. With the polynomial reproducing kernel ψ, we compute the moments μ_m defined in (9). We obtain the annihilation filter h_m by solving the linear system of equations: $\mathrm{T}(\mu_{\mathbf{m}})\mathbf{h} = \mathbf{0}$. The Dirac locations can be uniquely retrieved from the roots of the filter coefficients. The amplitudes are then obtained by performing fitting on the moment expression in (9).

Fig. 1 describes the signal reconstruction process. An algorithmic implementation is provided in Algorithm. 1.

Algorithm 1 Sparse Signal Recovery for Modulo Sampling

Input: Dual-channel Modulo Samples $y_{\lambda_1}[n], y_{\lambda_2}[n]$

Compute the residue difference $\underline{r}_{\lambda_{1,2}}$.
for $i = 0$ to $L_1 + L_2 - 1$ **do**
  Find the integers $\{p_l, q_l\}$ that satisfies that $c_l = 2\lambda_2 p_l - 2\lambda_1 q_l, (p_l, q_l) \in \mathbb{Z}^2$.
end for
Recover the residue $\underline{\varepsilon}^g_{\lambda_1}[n], \underline{\varepsilon}^g_{\lambda_2}[n]$. The sparse samples $g[n]$ can be reconstructed by applying the anti-difference operator Δ^{-1}.
Compute the moments μ_m and obtain the annihilation filter h_m by solving (10).
Compute the locations t_k by finding the roots of $\widehat{h}(z)$ and amplitudes from least-square fitting on (9).

Output: The reconstructed sparse signal $g(t)$.

6. NUMERICAL EXPERIMENTS

The proposed signal recovery method in Algorithm. 1 performs up to machine precision with computer simulations. To demonstrate this, we setup the following tests as shown in Fig. 3 and Fig. 4: $g(t)$ is composed of $K = 3$ Diracs with randomly generated (normal distribution) locations and amplitudes. The sampling kernel ψ is a B-spline with $P = 7$. The dynamic range $\|g\|_\infty$ in Fig. 3 and Fig. 4 is $50.0\lambda_1, 70.7\lambda_2$ and $51.1\lambda_1, 71.2\lambda_2$, respectively. We use $N = 19$ samples for each numerical experiments.

We use the mean-squared error (MSE) between the filtered signal $\{g(nT)\}_{n=0}^{N-1}$ and its reconstruction to evaluate the algorithm performance. In both examples, the high dynamic range leads to $L_1 = L_2 = 10$ in Fig. 3; $L_1 = L_2 = 7$ in Fig. 4. Despite the high dynamic range, the proposed algorithm achieves an accurate recovery up to machine precision (MSE $= 1.19 \times 10^{-16}$) in Fig. 3.

In order to demonstrate the super-resolution capability, we consider the case of closely-located spikes,

$$t_k = \begin{bmatrix} -1.62 & 0.71 & 0.81 \end{bmatrix}^\top.$$

In particular, resolving t_1 and t_2 can be challenging with conventional (non-modulo) samples, the challenge is further intensified with modulo sampling due to the non-linear nature of acquisition. Despite this, our algorithm can resolve the spikes up to machine precision.

7. CONCLUSION

In this paper, we propose a novel, *dual-channel* sampling pipeline which enables a perfect recovery of time-limited signals. Our approach can handle non-bandlimited functions and the construction of the acquisition architecture allows for a recovery principle that does not depend on sampling rate. Our work also considers that super-resolution scenario of closely spaced spikes. Developing reconstruction algorithms that can tackle quantization and system noise remains an integral part of our future work.

8. REFERENCES

[1] M. Unser, "Sampling-50 years after Shannon," *Proc. IEEE*, vol. 88, no. 4, pp. 569–587, Apr. 2000.

[2] A. Bhandari, F. Krahmer, and R. Raskar, "On unlimited sampling," in *IEEE Intl. Conf. on Sampling Theory and Applications (SampTA)*. IEEE, Jul. 2017.

[3] ——, "On unlimited sampling and reconstruction," *IEEE Trans. Signal Process.*, vol. 69, pp. 3827–3839, Dec. 2021.

[4] ——, "Methods and apparatus for modulo sampling and recovery," US Patent US10 651 865B2, May, 2020.

[5] A. Bhandari, F. Krahmer, and T. Poskitt, "Unlimited sampling from theory to practice: Fourier-Prony recovery and prototype ADC," *IEEE Trans. Signal Process.*, vol. 70, pp. 1131–1141, Sep. 2021.

[6] A. Bhandari, "Back in the US-SR: Unlimited sampling and sparse super-resolution with its hardware validation," *IEEE Signal Process. Lett.*, vol. 29, pp. 1047–1051, Mar. 2022.

[7] D. Florescu, F. Krahmer, and A. Bhandari, "The surprising benefits of hysteresis in unlimited sampling: Theory, algorithms and experiments," *IEEE Trans. Signal Process.*, vol. 70, pp. 616–630, Jan. 2022.

[8] T. Feuillen, B. M. Shankar, and A. Bhandari, "Unlimited sampling radar: Life below the quantization noise," in *(to appear) IEEE Intl. Conf. on Acoustics, Speech and Signal Processing (ICASSP)*, Mar. 2023.

[9] S. Fernandez-Menduina, F. Krahmer, G. Leus, and A. Bhandari, "Computational array signal processing via modulo nonlinearities," *IEEE Trans. Signal Process.*, vol. 70, pp. 2168–2179, Mar. 2022.

[10] A. Bhandari, F. Krahmer, and R. Raskar, "Unlimited sampling of sparse signals," in *IEEE Intl. Conf. on Acoustics, Speech and Signal Processing (ICASSP)*. IEEE, Apr. 2018.

[11] A. Bhandari and F. Krahmer, "HDR imaging from quantization noise," in *IEEE Intl. Conf. on Image Processing (ICIP)*. IEEE, Oct. 2020.

[12] M. Beckmann, A. Bhandari, and F. Krahmer, "The modulo Radon transform: Theory, algorithms, and applications," *SIAM J Imaging Sci*, vol. 15, no. 2, pp. 455–490, Apr. 2022.

[13] Z. Liu, A. Bhandari, and B. Clerckx, "λ-MIMO: Massive MIMO via modulo sampling," arXiv:2210.10193, Oct. 2022.

[14] S. Rudresh, A. Adiga, B. A. Shenoy, and C. S. Seelamantula, "Wavelet-based reconstruction for unlimited sampling," in *IEEE Intl. Conf. on Acoustics, Speech and Signal Processing (ICASSP)*. IEEE, Apr. 2018.

[15] Y. Gong, L. Gan, and H. Liu, "Multi-channel modulo samplers constructed from gaussian integers," *IEEE Signal Process. Lett.*, vol. 28, pp. 1828–1832, Aug. 2021.

[16] E. Romanov and O. Ordentlich, "Above the nyquist rate, modulo folding does not hurt," *IEEE Signal Process. Lett.*, vol. 26, no. 8, pp. 1167–1171, Aug. 2019.

[17] A. Weiss, E. Huang, O. Ordentlich, and G. W. Wornell, "Blind modulo analog-to-digital conversion of vector processes," in *IEEE Intl. Conf. on Acoustics, Speech and Signal Processing (ICASSP)*. IEEE, May 2022.

[18] E. Azar, S. Mulleti, and Y. C. Eldar, "Residual recovery algorithm for modulo sampling," in *IEEE Intl. Conf. on Acoustics, Speech and Signal Processing (ICASSP)*. IEEE, May 2022.

[19] M. Vetterli, P. Marziliano, and T. Blu, "Sampling signals with finite rate of innovation," *IEEE Trans. Signal Process.*, vol. 50, no. 6, pp. 1417–1428, Jun. 2002.

[20] P. L. Dragotti, M. Vetterli, and T. Blu, "Sampling moments and reconstructing signals of finite rate of innovation: Shannon meets strang–fix," *IEEE Trans. Signal Process.*, vol. 55, no. 5, pp. 1741–1757, May 2007.

[21] T. Blu, P.-L. Dragotti, M. Vetterli, P. Marziliano, and L. Coulot, "Sparse sampling of signal innovations," *IEEE Signal Process. Mag.*, vol. 25, no. 2, pp. 31–40, Mar. 2008.

[22] O. Musa, P. Jung, and N. Goertz, "Generalized approximate message passing for unlimited sampling of sparse signals," in *IEEE Intl. Conf. on Signal and Information Processing (GlobalSIP)*. IEEE, Nov. 2018.

[23] V. Shah and C. Hegde, "Sparse signal recovery from modulo observations," *EURASIP Journal on Advances in Signal Processing*, vol. 2021, no. 1, Apr. 2021.

[24] D. Prasanna, C. Sriram, and C. R. Murthy, "On the identifiability of sparse vectors from modulo compressed sensing measurements," *IEEE Signal Process. Lett.*, vol. 28, pp. 131–134, Dec. 2021.